

Rapid synthesis of dense Ti_3SiC_2 by spark plasma sintering

N.F. Gao^a, J.T. Li^b, D. Zhang^c, Y. Miyamoto^{a,*}

^aJoining and Welding Research Institute, Osaka University, Ibaraki, Osaka 5670047, Japan

^bLaboratory of Special Ceramics & P/M, University of Science and Technology Beijing, Beijing 100083, PR China

^cState Key Laboratory of Metal Matrix Composites, Shanghai Jiao Tong University, No. 1954 Huashan Rd., Shanghai 200030, PR China

Received 24 September 2001; received in revised form 21 December 2001; accepted 12 January 2002

Abstract

Ti_3SiC_2 was rapidly synthesized and simultaneously consolidated from the starting mixture of Ti/Si/2TiC by spark plasma sintering (SPS). An intensive reaction leading to the formation of Ti_3SiC_2 occurred at the measured temperature of around 1200 °C, which is several hundreds degrees lower than that of conventional reactive hot pressing. The phase composition of the product could be tailored by adjusting the process parameters. An axisymmetric preferred orientation of the Ti_3SiC_2 grains with well-developed (008) planes was formed, resulting in an anisotropic hardness in respect to the textured product. © 2002 Elsevier Science Ltd. All rights reserved.

Keywords: Mechanical properties; Microstructure-final; Reactive synthesis; Ti_3SiC_2 ; X-ray diffraction; SPS

1. Introduction

Ti_3SiC_2 is a unique ceramic because of its low hardness, high Young's modulus, excellent thermal shock resistance, and high electrical conductivity.¹ Many attempts have been made to fabricate bulk Ti_3SiC_2 during the past decade by combustion synthesis,^{2–5} reactive sintering,^{6–9} reactive hot pressing,¹⁰ reactive hot isostatic pressing (HIP),^{11,12} and other methods. However, it is difficult to obtain a single phase product because of the narrow stable region of Ti_3SiC_2 in the ternary phase diagram of the Ti–Si–C system. Barsoum et al. have successfully fabricated high-purity polycrystalline Ti_3SiC_2 from 3Ti/SiC/C powders by reactive hot pressing at 1600 °C, 40 MPa for 4 h.¹⁰ The secondary phases were less than 2 vol.% SiC and TiC_x in the final products. Some investigations on the phase diagram of the Ti–Si–C system showed that the stable region of Ti_3SiC_2 lies in the temperature range of 1100–1400 °C.^{13,14} A high sintering temperature causes grain coarsening, resulting in the deterioration of mechanical properties of Ti_3SiC_2 .

Recently, a novel sintering technique called spark plasma sintering (SPS)^{15–18} or plasma activated sintering (PAS)^{19–21} has emerged as a versatile technique to rapidly sinter a number of materials including metals, ceramics, polymers, and composites in a period of minutes. In this method, as-received powders are placed in a graphite die, pressed uniaxially, and then heated by passing a high pulsed current through the powders and/or the die. Sintering occurs within minutes. It is suggested that electro-discharging among particles can activate the particle surface and assist sintering.¹⁵ There are many reports on the sintering of as-received ceramic or metal powders by SPS, but few on materials synthesis and densification in one step.

In our previous work, high-purity Ti_3SiC_2 powders were synthesized successfully by reactive sintering of Ti/Si/2TiC at temperatures as low as 1415 °C.²² Dense polycrystalline Ti_3SiC_2 of high purity was obtained by reactively hot isostatic pressing of Ti/Si/2TiC powders at 1415 °C, 100 MPa for 2 h.²³ Based on these results, in combination with the advantages of the SPS process, the purpose of this study is to obtain high-purity and dense Ti_3SiC_2 with a fine-grained structure at lower temperatures in a short time. The synthesis and densification behavior of Ti_3SiC_2 during the SPS process, as well as the microstructure development, were studied. Several mechanical properties were also measured.

* Corresponding author. Tel.: +81-6-6879-8693; fax: +81-6-6879-8693.

E-mail address: miyamoto@jwri.osaka-u.ac.jp (Y. Miyamoto).

2. Experimental procedure

Commercially available powders of Ti (<45 μm , 99.7% purity, Sumitomo Sitix, Co. Ltd., Japan), Si (<10 μm , 99.9% purity, High Purity Chemicals Co. Ltd., Japan), and TiC (1.7 μm , 99.2% purity, Nihon New Metals Co. Ltd., Japan) were used as the raw materials. The Ti, Si and TiC powders were mixed in a stoichiometric molar ratio of 1:1:2 in ethanol by SiC ball milling, and then dried in vacuum. The mixtures were loosely compacted into a graphite die of 20 or 30 mm in diameter and sintered in vacuum (1 Pa) at various temperatures (1125–1400 $^{\circ}\text{C}$) using an SPS apparatus (Dr. SINTER, SPS-1050, Sumitomo Coal Mining Co. Ltd., Japan). A constant heating rate of 100 $^{\circ}\text{C}/\text{min}$ was employed, while the applied pressure was varied from 20 to 60 MPa. The on/off time ratio of the pulsed current was set to 12/2 in each run. The maximum current reached approximately 3000 A during sintering. The soaking time at high temperatures was within 10 min. The upper ram of the SPS apparatus was fixed, while the displacement of the shifting lower press ram was recorded in order to analyze the synthesis and sintering behavior.

The sintered sample was polished and the density was determined by Archimedes' method using water immersion. The phase identification and the preferred orientation of the Ti_3SiC_2 crystalline grains were evaluated by X-ray diffraction analysis using $\text{Cu } K_{\alpha}$ radiation. The secondary phase content of TiC_x was calculated according to the calibration line.²⁴ The microstructure of the sample was observed by SEM. The product was cut along the cylindrical axis into two pieces. The microhardness at the top surface and the lateral surface were measured by a diamond Vickers hardness tester. The indentation loads, ranging from 10 to 500 N, were applied for 15 s for each measurement.

3. Results

The sintered samples consisted mainly of Ti_3SiC_2 . Some secondary phases, such as TiC_x and $\text{Ti}_5\text{Si}_3\text{C}_x$, appeared depending on the sintering temperature. X-ray diffraction patterns of samples sintered at 20 MPa pressure at various temperatures are shown in Fig. 1. Fig. 2 shows the TiC_x content as a function of sintering temperature, which was reduced to 5 wt.% when sintered at 1200 $^{\circ}\text{C}$ for 5 min at 20 MPa pressure.

Fig. 3 shows the displacement of the lower press ram as a function of sintering temperature when the press load was kept at 20 MPa. The lower press ram went up as the temperature increased to ~ 1200 $^{\circ}\text{C}$, but went down at higher temperatures. This behavior suggests that the volume of the powder compact shrunk continuously with temperature, but changed to expansion

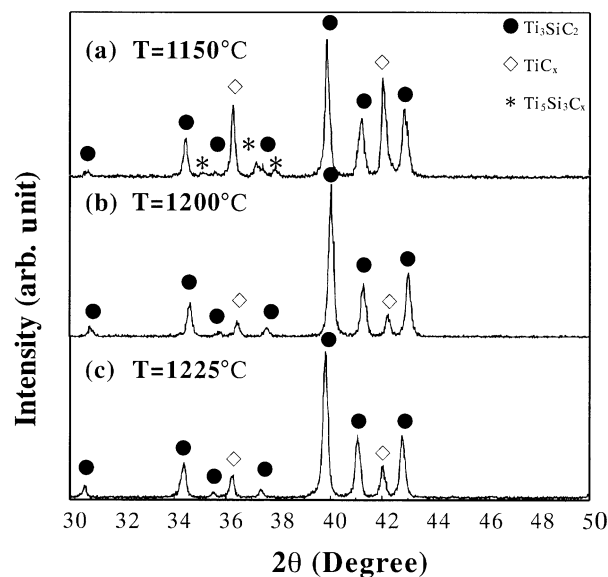


Fig. 1. XRD patterns of SPS products sintered at different temperatures.

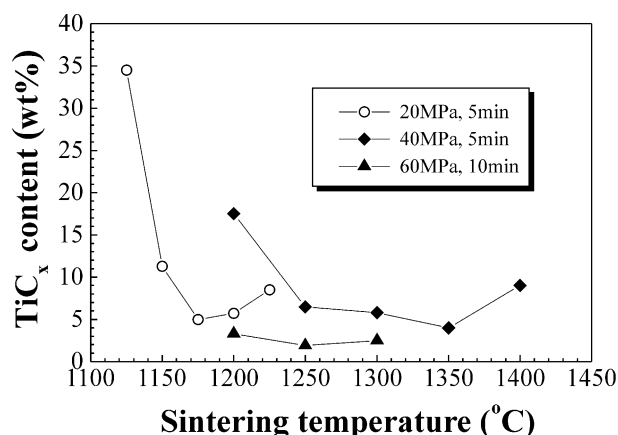


Fig. 2. The TiC_x content of as-synthesized samples as a function of sintering temperature.

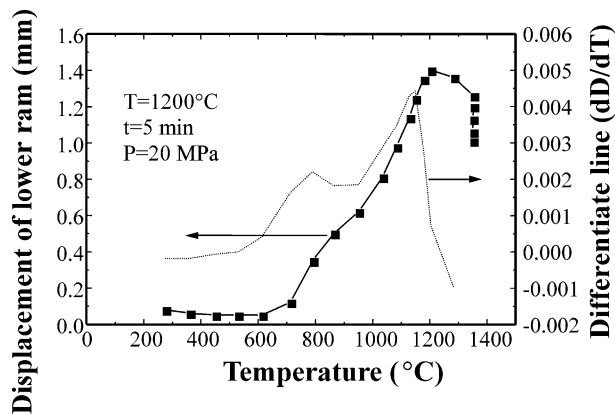


Fig. 3. Dependence of the displacement of a lower press ram on the sintering temperature during SPS run under a pressure of 20 MPa.

at $\sim 1200^\circ\text{C}$. The formation of Ti_3SiC_2 seems to produce this volume expansion. Fig. 4 shows the fine-grained structure of the top surface for the sample sintered at 1200°C , 20 MPa for 5 min after etching by an $\text{HF}:\text{HNO}_3$ aqueous solution. The average grain size of Ti_3SiC_2 is below $10\ \mu\text{m}$. TiC_x (shown as a bright contrast) is about $1\text{--}2\ \mu\text{m}$ size, which is near the original TiC_x particle size in the as-received powders. Large pores of black contrast about the size of $10\ \mu\text{m}$ were produced at the locations where the $\text{Ti}_5\text{Si}_3\text{C}_x$ existed after etching. Some closed pores inside the Ti_3SiC_2 grains can also be seen, which would be attributed to the short sintering time. Fig. 5 shows the hardness as a function of the applied indentation load for the same sample. At higher loads, the microhardness reaches a constant value of 3.2 GPa. Barsoum and El-Raghy et al. took the low hardness as indirect evidence of the purity of the as-synthesized Ti_3SiC_2 .^{1–25} In the present study, the low hardness of the SPS synthesized sample containing 5 wt.% TiC_x may be attributed to its low density (95% of theoretical).

Fig. 6 plots the temperature at which the extensive volume expansion occurred as a function of the loading

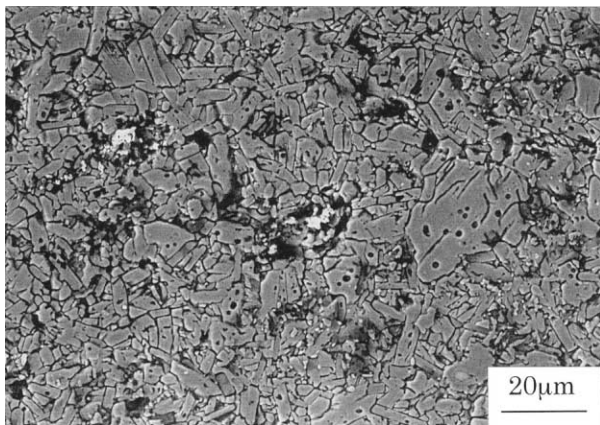


Fig. 4. SEM micrograph of the polished and etched surface for the sample sintered at 1200°C , 20 MPa for 5 min.

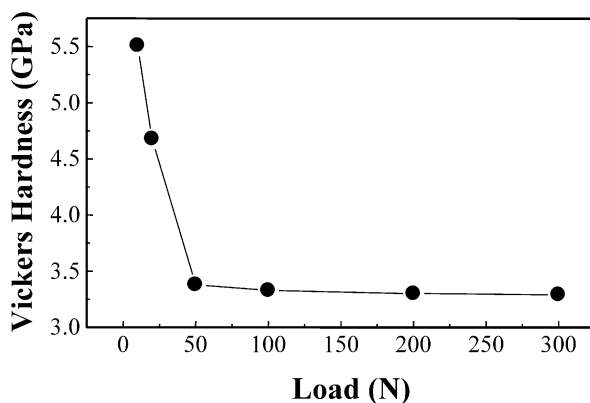


Fig. 5. Vickers hardness versus indentation load for the sample sintered 1200°C , 20 MPa for 5 min.

pressure. The temperature increased with an increase in the press load. When SPS was carried out under a pressure of 60 MPa, the obtained product was almost fully densified, though a small quantity of TiSi_2 phase appeared besides the Ti_3SiC_2 and TiC_x . The TiC_x contents were plotted for different pressure and time conditions of the SPS process as shown in Fig. 2. The best product contained 2 wt.% TiC_x , which was sintered at 1250°C , 60 MPa for 10 min. This temperature is 350°C lower than that of reactive hot pressing.¹⁰ The electro-discharge among powders may lead to self-heating and purification of the particle surface, resulting in activation of the formation for Ti_3SiC_2 .¹⁵

Fig. 7 shows X-ray diffraction patterns of the products prepared at 1350 and 1400°C under 40 MPa pressure. The TiSi_2 content slightly increased at 1400°C . The tendency of Ti_3SiC_2 to decompose into TiSi_2 at

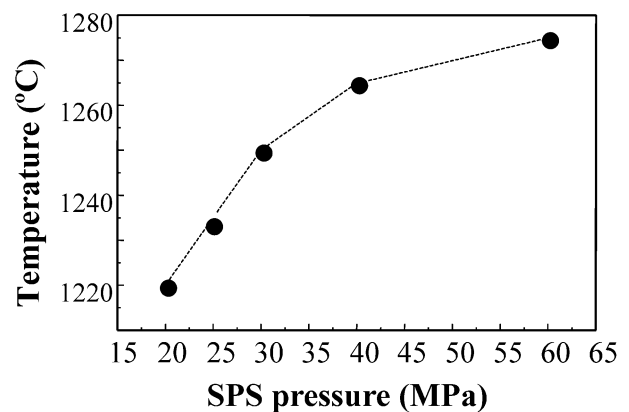


Fig. 6. Variation of temperature corresponding to the expansion of the compacted materials as a function of the SPS pressure.

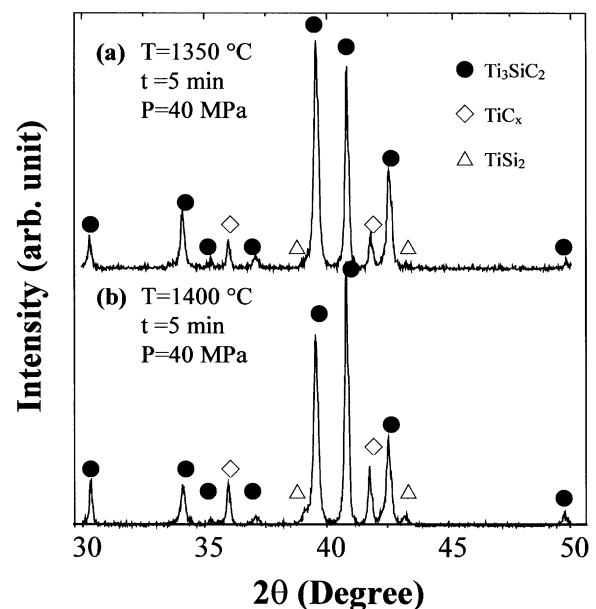


Fig. 7. X-ray diffraction patterns of SPS samples sintered at (a) 1350°C and (b) 1400°C under 40 MPa pressure, respectively.

high temperature is also in agreement with the observation of the increasing TiSi_2 content after HIPing the combustion derived Ti_3SiC_2 powder.²⁴

When the graphite die diameter was increased from 20 to 30 mm, the TiC_x content could be controlled to 2 wt.% when sintered at 1250 °C for 10 min under 60 MPa pressure. The sample was cut along the cylindrical axis into two pieces. X-ray diffraction analyses on the top and lateral surfaces were carried out. The pulverized sample was also analyzed by X-ray diffraction. Fig. 8 shows the XRD pattern on the top surface. The strongest diffraction peak changed from (104) plane on both surfaces to that of (008) plane on the pulverized sample. The peak intensity of (104) plane on the lateral surface is higher than that on the top surface. These results suggest that Ti_3SiC_2 grains grew preferentially with the basal planes rotating towards the loading direction. The anisotropic grain growth is also observed on the fracture surface, as shown in Fig. 9. The Ti_3SiC_2 typical grains have a thin plate-like form with a diameter of 10–30 μm and a thickness of 3–6 μm . These

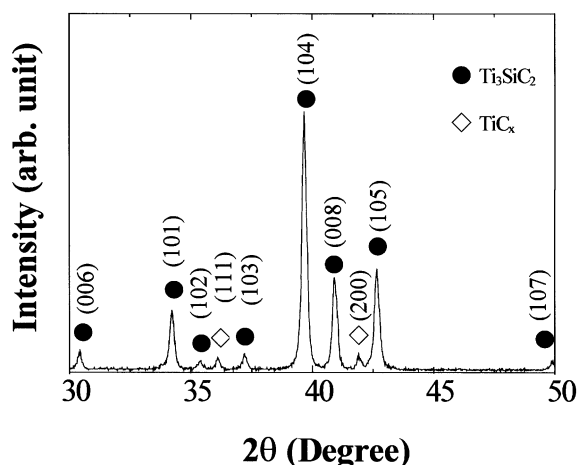


Fig. 8. X-ray diffraction pattern on the top surface of the sample sintered at 1250 °C, 60 MPa for 10 min using a 30-mm diameter die.

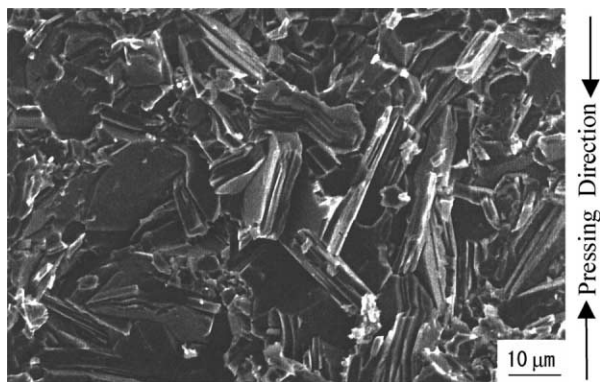


Fig. 9. SEM micrograph of the fracture surface of the Ti_3SiC_2 sintered at 1250 °C, 60 MPa for 10 min using a 30-mm diameter die, where the preferential orientation is observed.

grain sizes are one order smaller than those of materials prepared by other methods.²⁶ It has been well established by TEM observation that the platelet grains are parallel to the (001) plane and perpendicular to the c-axis of the Ti_3SiC_2 crystal structure.¹¹ The platelet Ti_3SiC_2 grains tended to be parallel to the pressing direction.

The hardness of the same sample exhibited an anisotropic behavior as shown in Fig. 10. On the top surface, the hardness, H_{V_t} , decreased sharply at a load between 10 and 50 N and then decreased gradually at higher loads as already indicated in a previous report.¹¹ On the lateral surface, the hardness, H_{V_l} , showed less dependence on the indentation load and lower values than H_{V_t} at all load levels. The corresponding SEM micrographs around the indentation marks at the top and lateral surfaces show the lateral cracks extension from the indentation mark on the top surface, but not in the case on the lateral surface. It is suggested that on the lateral surface the indentation load may act as a force to delaminate the platelet Ti_3SiC_2 in the weak Si bonding direction. Due to the energy dissipation in this process, a higher toughness and a lower hardness exhibited on the lateral surface as a result of the anisotropy caused by the preferential grain growth.

4. Discussion

In spark plasma sintering, raw powders were compacted in a press and heated by passing through several thousands ampere of pulsed current through die and powders. In the current understanding of the SPS process, it is assumed that the densification is achieved by the contribution of three factors: plasma generation, resistance heating and pressure application.^{15–21} However, the studies of the plasma effects on sintering are

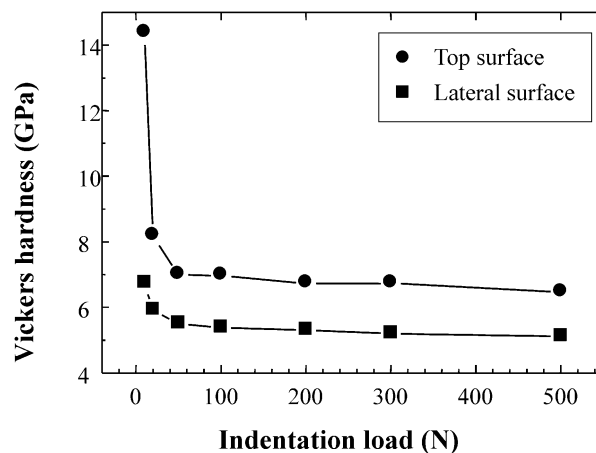


Fig. 10. Vickers hardness of as-synthesized Ti_3SiC_2 a 30-mm diameter die as a function of indentation load, measured along different directions.

very limited. Some researchers suggested that the plasma is enhanced at the initial stage of sintering because there are many small gaps and contact points among the powder particles. The plasma is reduced gradually as the number of gaps or pores decrease.

The SPS method is an efficient way for the synthesis and simultaneous densification of Ti_3SiC_2 at a relatively low temperature in a soaking duration of minutes. Firstly, the formation of Ti_3SiC_2 is highly enhanced by the above-mentioned effects of plasma generation, surface purification, and resistance heating in the SPS process. Secondly, the synthesis of Ti_3SiC_2 is probably quickened by using the Ti/Si/2TiC powders due to the inclusion of Si to form the Ti-Si liquid phase, which may accelerate the diffusion-controlled reaction process as compared with the 3Ti/SiC/C powders.²⁷

The preferential grain growth of Ti_3SiC_2 along the basal plane during reactive sintering of 3Ti/SiC/C took place when the heating rate was raised to over 12°C/min and the combustion reactions were induced.²⁸ It seems that the higher heating rate, and concomitantly, the rapid formation of Ti_3SiC_2 , would favor the preferential grain growth along the crystallographic basal planes. In the present experiment, a heating rate as high as 100°C/min was employed. It is reasonable to expect the same combustion-like reaction took place in the Ti/Si/2TiC system,²⁹ thus Ti_3SiC_2 with well-developed basal planes might be obtained. From Fig. 9, it is evident that the platelet Ti_3SiC_2 grains are inclined to align not parallel to the top surface but perpendicular to the lateral surface of the bulk product. The textured Ti_3SiC_2 is of great technical importance as indicated by Barsoum et al. because such highly oriented Ti_3SiC_2 bulk material exhibited some form of plasticity at room temperature under compression.³⁰ This textured microstructure is responsible for the anisotropic hardness and toughness of the as-synthesized Ti_3SiC_2 . The reason for the formation of the textured microstructure may be attributed to the shear stress in the liquid phase during uniaxial loading, which causes the platelet Ti_3SiC_2 to become aligned along the pressing direction. On the other hand, the exertion of the shear stress may also accelerate the grain growth of Ti_3SiC_2 along the basal plane.

5. Conclusions

Simultaneous synthesis and densification of Ti_3SiC_2 was rapidly achieved by spark plasma sintering of Ti/Si/2TiC powder mixtures. Ti_3SiC_2 with 2 wt.% TiC_x was produced in the sintering temperature range of $1250\text{--}1300^\circ\text{C}$, depending on the applied pressure and the dimension of the sample. Preferential grain growth of Ti_3SiC_2 along the crystallographic basal plane was detected by XRD analysis. Because these platelet grains

tended to align perpendicular to the loading surface, an anisotropic hardness was obtained.

References

1. Barsoum, M. W. and El-Raghy, T., A progress report on Ti_3SiC_2 , Ti_3GeC_2 , and the H-Phases, M_2BX . *J. Mater. Synth. Proc.*, 1997, **5**, 197–216.
2. Lis, J., Miyamoto, Y., Pampuch, R. and Tanihata, K., Ti_3SiC_2 -based materials prepared by HIP-SHS techniques. *Mater. Lett.*, 1995, **22**, 163–168.
3. Klemm, H., Tanihata, K. and Miyamoto, Y., Gas pressure combustion and hot isostatic pressing in the Ti-Si-C System. *J. Mater. Sci.*, 1993, **28**, 1557–1562.
4. Pampuch, R., Lis, J. and Stobierski, L., Ti_3SiC_2 -based materials produced by self-propagating high-temperature synthesis (SHS) and ceramic processing. *J. Mater. Synth. Proc.*, 1993, **1**, 93–100.
5. Pampuch, R., Lis, J., Stobierski, L. and Tymkiewicz, M., Solid combustion synthesis of Ti_3SiC_2 . *J. Eur. Ceram. Soc.*, 1989, **5**, 283–287.
6. Okano, T., Yano, T. and Iseki, T., Synthesis and mechanical properties of Ti_3SiC_2 ceramic. *Trans. Met. Soc. Jap.*, 1993, **14A**, 597–600.
7. Tong, X., Okano, T., Iseki, T. and Yano, Y., Synthesis and high temperature mechanical properties of $\text{Ti}_3\text{SiC}_2/\text{SiC}$. *J. Mater. Sci.*, 1995, **30**, 3087–3090.
8. Radhakrishnan, R., Henagar, C. H. Jr., Brimhall, J. L. and Bhaduri, S. B., Synthesis and characterization of $\text{Ti}_3\text{SiC}_2/\text{SiC}$ and TiSi_2/SiC composites using displacement reactions in the Ti-Si-C System. *Ser. Mater. Metall.*, 1996, **34**, 1809–1814.
9. Racault, C., Langlais, F. and Naslain, R., Solid state synthesis and characterization of the ternary phase Ti_3SiC_2 . *J. Mater. Sci.*, 1994, **29**, 3384–3392.
10. Barsoum, M. W. and El-Raghy, T., Synthesis and characterization of a remarkable ceramic: Ti_3SiC_2 . *J. Am. Ceram. Soc.*, 1996, **79**, 1953–1956.
11. Gao, N. F., Miyamoto, Y. and Zhang, D., Dense Ti_3SiC_2 prepared by reactive HIP. *J. Mater. Sci.*, 1999, **34**, 4385–4392.
12. Li, J. F., Sato, F. and Watanabe, R., Synthesis of Ti_3SiC_2 polycrystals by hot isostatic pressing of the elemental powders. *J. Mater. Sci. Lett.*, 1999, **18**, 1595–1597.
13. Wakelkamp, W. J. J., van Loo, F. J. and Metselaar, R., Phase relations in the Ti-Si-C system. *J. Eur. Ceram. Soc.*, 1991, **8**, 135–139.
14. Naka, M., Feng, J. C. and Schuster, J. C., Phase reaction paths for the SiC/Ti system. *Met. Mater. Trans.*, 1997, **28A**, 1385–1390.
15. Tokita, M. Mechanism of spark plasma sintering. In *Proceedings of the International Symposium on Microwave, Plasma and Thermochemical Processing of Advanced Materials*, ed S. Miyake and M. Samandi. JWRI, Osaka Universities Japan, 1997, pp. 69–76.
16. Nishimura, T., Mitomo, M., Hirotsuru, H. and Kawahara, M., Fabrication of silicon nitride nano-ceramics by spark plasma sintering. *J. Mater. Sci. Lett.*, 1995, **14**, 1046–1047.
17. Omori, M., Sakai, H., Okubo, A. and Hirai T., Preparation of stainless steel/ $\text{ZrO}_2(3Y)$ functional gradient material, In *Proceedings of the 3rd Int. Symp. On Structural and Functional Gradient Materials*, ed Cherradi N. and Ilschner B. Presses polytechniques et universitaires romandes. Lausanne, Switzerland, 1995, pp. 65–70.
18. Omori, M., Okubo, A., Gilhwan, K. and Hirai, T., Consolidation of thermosetting polyimide by the spark plasma system. *J. Mater. Synth. Proc.*, 1997, **5(4)**, 279–282.
19. Risbud, S. H. and Groza, J. R., Clean grain boundaries in an aluminum nitride ceramic densified without additives by a

- plasma-activated sintering process. *Philos. Mag.*, 1994, **69**(3), 525–533.
20. Schneider, J. A., Risbud, S. H. and Mukherjee, A. K., Rapid consolidation processing of silicon nitride powders. *J. Mater. Res.*, 1996, **11**(2), 358–362.
21. Tracy, M. J. and Groza, J. R., Consolidation of nanocrystalline Nb-Al powders by plasma activated sintering. *Nanostruct. Mater.*, 1993, **2**, 441–449.
22. Li, J. T. and Miyamoto, Y., Fabrication of monolithic Ti_3SiC_2 ceramic through reactive sintering of Ti/Si/2TiC. *J. Mater. Synth. Proc.*, 1999, **7**(2), 91–96.
23. Gao, N. F., Miyamoto, Y. and Zhang, D., On physical and thermochemical properties of high-purity Ti_3SiC_2 . *Mater. Lett.*, in press.
24. Gao, N. F., Miyamoto, Y. and Tanihata, K., Synthesis of highly dense Ti_3SiC_2 by HIP and its characterization. *J. Soc. Mater. Sci. Jpn.*, 1998, **47**, 994–999.
25. El-Raghy, T., Zavaliangous, A., Barsoum, M. W. and Kalidindi, S. R., Damage mechanisms around hardness indentations in Ti_3SiC_2 . *J. Am. Ceram. Soc.*, 1997, **80**(2), 513–516.
26. Low, I. M., Lee, S. K., Lawn, B. R. and Barsoum, M. W., Contact damage accumulation in Ti_3SiC_2 . *J. Am. Ceram. Soc.*, 1998, **81**(1), 225–228.
27. Massalski, T. B., Murray, J. L., Bennet, L. H., Baker, H. and Kacprzaki, L., *Binary Alloy Phase Diagrams*, American Society for Metals. Materials Park, OH, 1986.
28. Li, J. T. and Miyamoto, Y., Investigation on novel features during reactive synthesis of Ti_3SiC_2 ceramic, In Proceedings of the First China Interanational Conference on High-performance Ceramics. In D. S. Yan and Z. D. Guan. Tsing Hua University Press, Beijing, 1999, pp. 594–597.
29. Trambukis, J. and Munir, Z. A., Effect of particle dispersion on the mechanism of combustion synthesis of titanium silicide. *J. Am. Ceram. Soc.*, 1990, **73**(5), 1240–1245.
30. Barsoum, M. W. and El-Raghy, T., Room temperature ductile carbides. *Met. Mater. Trans.*, 1999, **30A**, 363–369.